

Exact trapped N -soliton solutions of the nonlinear Schrödinger equation using the inverse problem method

Fred Cooper,^{1,2} Avinash Khare,³ John F. Dawson,⁴ Efsthios G. Charalampidis,⁵ and Avadh Saxena²

¹*Santa Fe Institute, 1399 Hyde Park Road, Santa Fe, NM 87501, USA*

²*Center for Nonlinear Studies and Theoretical Division, Los Alamos National Laboratory, Los Alamos, NM 87545, USA*

³*Physics Department, Savitribai Phule Pune University, Pune 411007, India*

⁴*Department of Physics, University of New Hampshire, Durham, NH 03824, USA*

⁵*Mathematics Department, California Polytechnic State University, San Luis Obispo, CA 93407-0403, USA*

(*Electronic mail: avadh@lanl.gov)

(*Electronic mail: echarala@calpoly.edu)

(*Electronic mail: john.dawson@unh.edu)

(*Electronic mail: avinashkhare45@gmail.com)

(*Electronic mail: cooper@santafe.edu)

(Dated: 24 October 2023, 1:30am PST)

In this work, we show the application of the “inverse problem” method to construct exact N trapped soliton-like solutions of the nonlinear Schrödinger or Gross-Pitaevskii equation (NLSE and GPE, respectively) in one, two, and three spatial dimensions. This method is capable of finding the external (confining) potentials which render specific assumed waveforms exact solutions of the NLSE for both attractive ($g < 0$) and repulsive ($g > 0$) self-interactions. For both signs of g , we discuss the stability with respect to self-similar deformations and translations. For $g < 0$, a critical mass M_c , or equivalently the number of particles, for instabilities to arise can often be found analytically. On the other hand, for the case with $g > 0$ corresponding to repulsive self interactions which is often discussed in the atomic physics realm of Bose-Einstein condensates (BEC), the bound solutions are found to be always stable. For $g < 0$, we also determine the critical mass numerically by using linear stability or Bogoliubov-de Gennes analysis, and compare these results with our analytic estimates. Various analytic forms for the trapped N -soliton solutions are discussed, including sums of Gaussians or higher-order eigenfunctions of the harmonic oscillator Hamiltonian.

Understanding the behavior of trapped atoms in BECs requires the numerical study of the existence, stability and spatio-temporal dynamics of solutions to the Gross-Pitaevskii equation (GPE). Exact solutions of the GPE subject to external potentials offers a path in which not only numerical simulations can be carried out for this purpose but analytical estimates for the stability of coherent structures can be derived. In this work, we consider the inverse problem method which is capable of determining suitable external potentials that make specified N -trapped soliton wave functions exact solutions to the GPE. The stability of these solutions is then studied using Derrick’s theorem and energy landscape techniques. We discuss potential realizations of trapped BECs in 1D, 2D, and 3D. Our theoretical results on stability analysis are compared with spectral computations in the realm of Bogoliubov-de Gennes analysis.

ubiquitous envelope equation arises in diverse physical contexts with a wide array of physical applications. Those include the description of the pulse propagation in nonlinear optical fibers^{2,3}, the evolution of the envelope of modulated wave groups^{4,5}, as well as the propagation of strongly dispersive waves in plasmas⁶, among many others. When the NLSE incorporates an external, i.e., confining potential, it is often called the Gross-Pitaevskii equation (GPE) which is a fundamental model for describing the static and dynamical properties of atomic Bose-Einstein condensation (BEC) in the mean-field approximation⁷⁻⁹. Indeed, solutions (either obtained analytically or numerically) of the related GPE in multiple well potentials are very useful in understanding the behavior of trapped atoms in BECs. Both signs of the self-interaction coupling constant can be implemented when studying BECs, by varying the external magnetic field near the Feshbach resonance¹⁰. Using such methods, attractive self-interaction solitons have been found in BECs¹¹.

There are various strategies for finding solutions to the NLSE for given external potentials. Indeed, and for a given potential, one may linearize the NLSE (i.e., upon neglecting the nonlinearity therein), and obtain an eigenvalue problem for the (discrete) energy levels (eigenvalues) and quantum states (eigenfunctions) of the system. The resulting problem

I. INTRODUCTION

The nonlinear Schrödinger equation (NLSE)¹ has arguably been the focal point of studies in nonlinear models because its

is of a Sturm-Liouville type, i.e., a linear Schrödinger equation, and may be solved either analytically¹² or numerically, see, e.g., Refs. 13 and 14. Its eigenvalues coincide with the values of the so called chemical potential⁹ at which nonlinear states bifurcate from. Then, for each eigenvalue (i.e., value of the chemical potential at the linear limit) and respective linear state, one can continue the latter towards the nonlinear regime by varying the chemical potential which itself controls the number of atoms in a BEC⁹. This departure from the linear limit is accomplished by using numerical continuation methods¹⁵. Another strategy for finding solutions to the NLSE revolves around starting with an approximate solution, and then varying the potential to find a solution.

In the present article, we depart from these strategies, and use the so-called “inverse problem” method. Within this method, one chooses beforehand a wave function that has to be an exact solution of the NLSE. This way, various external potentials can be constructed with an eye towards realizing them experimentally. This method has previously been used by Malomed and Stepanyants¹⁶ in the standard NLSE to determine potentials that have exact Gaussian-like solutions. It has also been used in Ref. 17 for potentials in the NLSE with arbitrary nonlinearity exponent. Recently, the authors of the present work have shown how to find confining potentials in the NLSE which lead to constant density, flat-top solitons in one, two, and three dimensions (denoted hereafter as 1D, 2D, and 3D, respectively)¹⁸. Herein, we consider wave function Ansätze corresponding to N -soliton pulses, and identify the respective potentials that make them exact solutions to the NLSE in 1D, 2D, and 3D. Moreover, and since the inverse problem method gives us exact solutions, we take this advantage in order to provide analytic estimates for the critical mass for attractive self-interaction solitons above which the soliton becomes unstable. Those are obtained by using Derrick’s theorem¹⁹, or by studying the energy landscape for translation deformations of the soliton¹⁷. We compare our analytical findings on stability and instability of the soliton solutions against linear stability considerations by using the Bogoliubov-de Gennes^{20,21} (BdG) method.

The paper is structured as follows. In Sec. II, we present the main setup of the inverse problem method together with the linear response equations. Multi-soliton solutions in 1D, 2D, and 3D are discussed in Sec. III together with their response under self-similar and translational deformations. In Sec. IV we study the linear response equations and compare our findings against numerical simulations. Finally, we state our conclusions in Sec. V.

II. INVERSE PROBLEM METHOD FOR THE CONFINING POTENTIAL AND THE LINEAR STABILITY OF THE SOLUTIONS

We consider herein a collection of particles with mass $m = 1/2$, and contact interaction strength g which is described by a classical action. Upon confining the particles with the introduction of an external potential denoted as $V(\mathbf{r}) \in \mathbb{R}$, the non-linear Schrödinger equation (NLSE) for this system⁹ is then

given by:

$$\{ -\nabla^2 + g |\psi(\mathbf{r}, t)|^2 + V(\mathbf{r}) \} \psi(\mathbf{r}, t) = i \partial_t \psi(\mathbf{r}, t), \quad (1)$$

where $\psi(\mathbf{r}, t)$ is a complex-valued function, i.e., $\psi(\mathbf{r}, t) \in \mathbb{C}$. Here we use units such that $\hbar = 1$ (see, also Ref. 18). It should be noted in passing that in the absence of the external potential (i.e., $V(\mathbf{r}) \equiv 0$), soliton solutions exist for both repulsive ($g > 0$) interactions (see Ref. 22), as well as attractive ($g < 0$) interactions (see Ref. 23).

Suppose that $u_0(\mathbf{r}) \in \mathbb{R}$ is the solution to Eq. (1) at $t = 0$. If we assume a time-dependent solution for $\psi(\mathbf{r}, t)$ given by the separation of variables ansatz:

$$\psi(\mathbf{r}, t) = u_0(\mathbf{r}) e^{-i\omega t}, \quad (2)$$

then Eq. (1) is written as:

$$\omega u_0(\mathbf{r}) + \nabla^2 u_0(\mathbf{r}) - g u_0^2(\mathbf{r}) u_0(\mathbf{r}) = V(\mathbf{r}) u_0(\mathbf{r}). \quad (3)$$

If we are considering the Gross-Pitaevskii equation (GPE)⁷⁻⁹ for BECs as a particular NLSE, then $\omega \rightarrow \mu_0$, where μ_0 is the chemical potential. (The connection between the NLSE and GPE is discussed among other places in Ref. 18.)

The potential that will make $\psi(\mathbf{r}, t) = u_0(\mathbf{r}) e^{-i\mu_0 t}$ an exact solution of the GPE is given by the (inverse) relation:

$$V(\mathbf{r}) = \mu_0 - g u_0^2(\mathbf{r}) + \frac{\nabla^2 u_0(\mathbf{r})}{u_0(\mathbf{r})}. \quad (4)$$

It is therefore the task of the experimenter to create such a potential. It is important to now regard the potential $V(\mathbf{r})$ as so constructed to be *external*, and is not varied with respect to $u_0(\mathbf{r})$. Since the potential is now fixed, the conserved energy is given by

$$E_0 = \int d^3x \left\{ [\nabla u_0(\mathbf{r})]^2 + \frac{g}{2} u_0^4(\mathbf{r}) + V(\mathbf{r}) u_0^2(\mathbf{r}) \right\}, \quad (5)$$

and the conserved norm which is related to the number of atoms in the BEC (see, Ref. 18) is given by

$$M = \int d^3x |\psi(\mathbf{r}, t)|^2. \quad (6)$$

Soliton wave functions in 1D, 2D, and 3D are discussed in Sec. III below.

The linear stability of such solutions in the constructed potential is found by expanding the solution $\psi(\mathbf{r}, t)$ in the form of power series in $\varepsilon (\ll 1)$:

$$\begin{aligned} \psi(\mathbf{r}, t) &= \psi_0(\mathbf{r}, t) + \varepsilon \phi(\mathbf{r}, t) + \dots \\ &= e^{-i\mu_0 t} u_0(\mathbf{r}) + \varepsilon \phi(\mathbf{r}, t) + \dots, \end{aligned} \quad (7)$$

where μ_0 is the chemical potential, and $u_0(\mathbf{r})$ is a particular solution of the time-independent GPE⁷⁻⁹. To first order in ε , $\phi(\mathbf{r}, t)$ and $\phi^*(\mathbf{r}, t)$ satisfy:

$$\begin{aligned} &\begin{pmatrix} [h(\mathbf{r}) + g u_0^2(\mathbf{r})] & g u_0^2(\mathbf{r}) \\ -g u_0^2(\mathbf{r}) & -[h(\mathbf{r}) + g u_0^2(\mathbf{r})] \end{pmatrix} \begin{pmatrix} \phi(\mathbf{r}, t) \\ \phi^*(\mathbf{r}, t) \end{pmatrix} \\ &= i \partial_t \begin{pmatrix} \phi(\mathbf{r}, t) \\ \phi^*(\mathbf{r}, t) \end{pmatrix}, \end{aligned} \quad (8)$$

where $h(\mathbf{r})$ is the Hermitian operator:

$$h(\mathbf{r}) = -\nabla^2 + V_0(\mathbf{r}), \quad (9)$$

$$V_0(\mathbf{r}) = V(\mathbf{r}) + gu_0^2(\mathbf{r}) = \mu_0 + \frac{\nabla^2 u_0(\mathbf{r})}{u_0(\mathbf{r})}. \quad (10)$$

Solutions to the linear response equations (8) are discussed in Sec. IV below.

III. MULTI-SOLITON SOLUTIONS

A. One dimension

Let us first choose for our two-trapped soliton wave function, the sum of two Gaussians in 1D. For this case, the solution $u_0(x)$ is given by

$$\begin{aligned} u_0(x) &= A_0 \left[e^{-a(x-q)^2/2} + e^{-a(x+q)^2/2} \right] \\ &= 2A_0 e^{-a(q^2+x^2)/2} \cosh(aqx). \end{aligned} \quad (11)$$

The conserved mass follows from Eq. (6), and gives

$$M_0 = \int_{-\infty}^{\infty} dx u_0^2(x) = 2\sqrt{\frac{\pi}{a}} (1 + e^{-aq^2}) A_0^2, \quad (12)$$

with the respective confining potential [cf. Eq. (4)] given by

$$V(x) = V_0(x) - gu_0^2(x), \quad (13a)$$

$$\begin{aligned} V_0(x) &= \mu_0 + u_0''(x)/u_0(x) \\ &= a^2 x(x - 2q \tanh(aqx)), \end{aligned} \quad (13b)$$

where we have chosen $\mu_0 = a(1 - aq^2)$ so that $V_0(0) = 0$. [The primes in Eq. (13b) stand for differentiation wrt x .] Plots of the density $\rho_0(x) = u_0^2(x)$ and the confining potential $V(x)$ are shown in the top and bottom panels of Fig. 1 as functions of x with parameter values $a = 1$, $q = 5$, and $M_0 = 10$ for $g = \pm 1$. We note that we have set the chemical potential $\mu_0 = -24$ so that $V(0) = 0$ therein. It can be discerned from the bottom panel of the figure that for this two-soliton ansatz, $V(x)$ consists of two near harmonic wells located at $x = \pm q$ when $g = 1$. On the other hand, and for $g = -1$, the potential contains two double-well potentials whose local maxima are located similarly at $x = \pm q$.

The odd two-Gaussian soliton, defined by

$$\begin{aligned} u_1(x) &= A_1 \left[e^{-a(x-q)^2/2} - e^{-a(x+q)^2/2} \right] \\ &= 2A_1 e^{-a(q^2+x^2)/2} \sinh(aqx) \end{aligned} \quad (14)$$

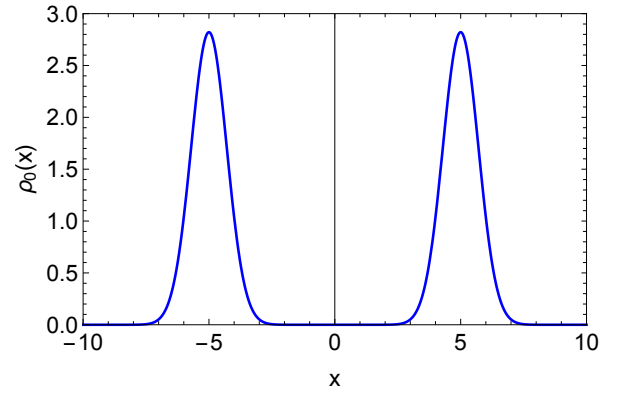
with conserved mass

$$M_1 = \int_{-\infty}^{\infty} dx u_1^2(x) = 2\sqrt{\frac{\pi}{a}} (1 - e^{-aq^2}) A_1^2, \quad (15)$$

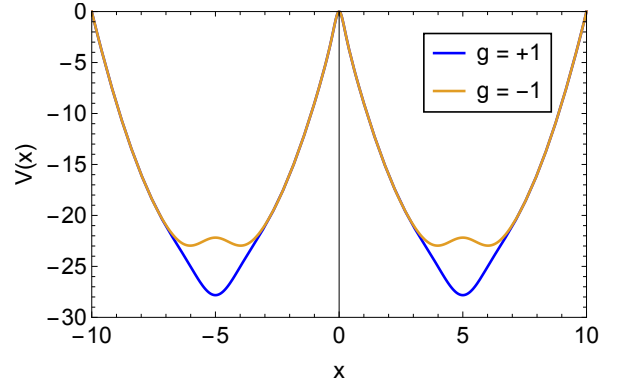
and confining potential given by

$$V(x) = V_1(x) - gu_1^2(x), \quad (16a)$$

$$\begin{aligned} V_1(x) &= \mu_0 + u_1''(x)/u_1(x) \\ &= a^2 x(x - 2q \coth(aqx)), \end{aligned} \quad (16b)$$



(a) $\rho_0(x)$



(b) $V(x)$

FIG. 1. Plot of the density $\rho_0(x)$ (top) and confining potential $V(x)$ (bottom) both as functions of x for $g = \pm 1$, and for the case when $a = 1$, $q = 5$, and $M_0 = 10$. The chemical potential is $\mu_0 = a(1 - aq^2) = -24$.

has nearly the same soliton density distribution for these parameters, and only a slightly different confining potential. Indeed, we compare $V_0(x)$ (even soliton) and $V_1(x)$ (odd soliton) in Fig. 2 [see, also, Eqs. (13b) and (16b)] which showcases that the only difference between them is the behavior near the origin. An experimenter would be hard pressed to construct potentials which would distinguish between even and odd solitons. The linear combinations

$$u_{\pm}(x) = [u_0(x) \pm u_1(x)]/2, \quad (17)$$

represent *single* solitons at $x = \pm q$. The creation of two solitons involves tunneling between the two harmonic wells. Similar results can be obtained by using $\text{sech}[a(q \pm x)]$ functions rather than Gaussian ones to construct two soliton densities.

Stability of these solutions with regard to width stretching can be studied using Derrick's theorem¹⁹. This theorem states that if the energy is a minimum under the transformation $x \rightarrow \beta x$, i.e., dilation, keeping the mass constant, the soliton is stable. The stretched wave function for the Gaussian case $u_0(x)$ then becomes:

$$u_s(x) = 2A_s e^{-a[q^2 + (\beta x)^2]/2} \cosh(aq\beta x), \quad (18)$$

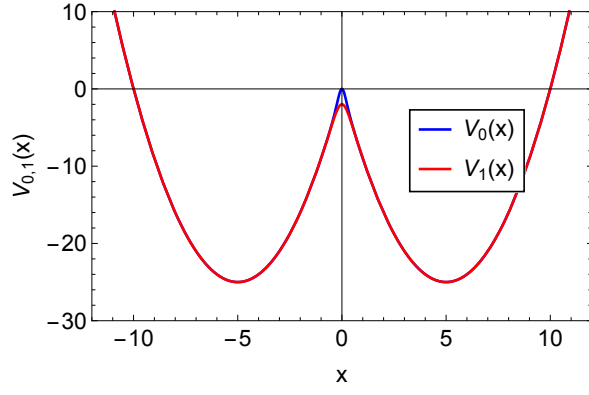


FIG. 2. Plots of $V_0(x)$ and $V_1(x)$ both as functions of x for the even and odd solitons that are given by Eqs. (13b) and (16b), respectively.

where now the mass is given by

$$M_0 = \int_{-\infty}^{\infty} dx u_s^2(x) = \frac{2}{\beta} \sqrt{\frac{\pi}{a}} (1 + e^{-aq^2}) A_s^2. \quad (19)$$

Defining $e_i(\beta) := E_i(\beta)/M_0$, the energy (5) is then the sum of three terms: $e(\beta) = e_1(\beta) + e_2(\beta) + e_3(\beta)$, where

$$e_1(\beta) = \frac{1}{M_0} \int dx u_s'^2(x) = \frac{a\beta^2}{2} \left[1 - \frac{2aq^2}{1 + e^{aq^2}} \right], \quad (20a)$$

$$e_2(\beta) = \frac{g}{2M_0} \int dx u_s^4(x) \quad (20b)$$

$$= \frac{gM_0\beta\sqrt{a}}{4\sqrt{2\pi}} \frac{(4e^{aq^2/2} + e^{2aq^2} + 3)}{(1 + e^{aq^2})^2},$$

$$e_3(\beta) = \frac{1}{M_0} \int dx V(x) u_s^2(x) \quad (20c)$$

$$= \frac{1}{M_0} \int dx [V_0(x) - g u_0^2(x)] u_s^2(x),$$

with $V_0(x)$ being given by (13b). We note in passing that unlike the integrals in Eqs. (20a) and (20b) which are evaluated explicitly, the integral in Eq. (20c) must be evaluated numerically. The top and bottom panels of Fig. 3 depict the energy $e(\beta)$ as a function of β for $g = 1$ (top panel) and $g = -1$ (bottom panel), respectively, with parameter values $a = 1$ and $q = 5$, and for several values of M_0 . It can be discerned from the top panel corresponding to the repulsive case (i.e., $g = 1$) that at $\beta = 1$, the soliton is always stable for all values of M_0 , however for the attractive case (i.e., $g = -1$), the soliton becomes unstable for $M_0 \approx 10$.

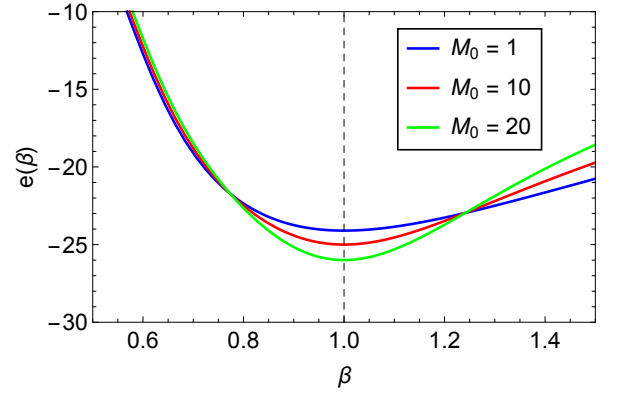
Translational stability can be studied by displacing the soliton solution $u_0(x)$ through the use of the transformation: $x \rightarrow x \pm \delta$. In this case, the trial wave function takes the form:

$$u_t(x) = A_t \left[e^{-a[x-\delta-q]^2/2} + e^{-a(x+\delta+q)^2/2} \right]$$

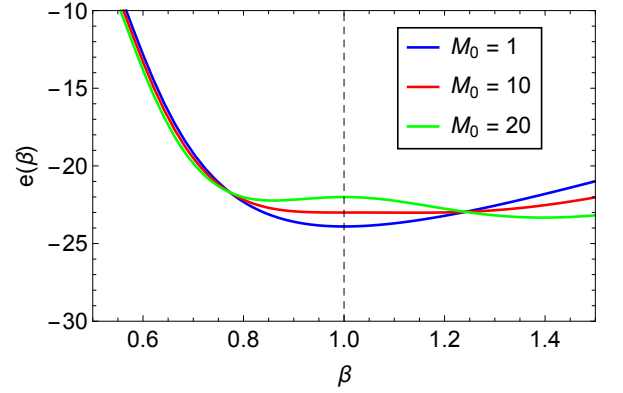
$$= 2A_t e^{-a[(q+\delta)^2+x^2]/2} \cosh[a(q+\delta)x], \quad (21)$$

where the mass is now given by

$$M_0 = \int_{-\infty}^{\infty} dx u_t^2(x) = 2\sqrt{\frac{\pi}{a}} (1 + e^{-a(q+\delta)^2}) A_t^2. \quad (22)$$



(a) $g = +1$



(b) $g = -1$

FIG. 3. Plots of energy $e(\beta)$ vs. β for $g = \pm 1$ for the case when $a = 1$ and $q = 5$. Note that the soliton for $g = 1$ is always stable whereas for $g = -1$, it becomes unstable for $M_0 \approx 10$.

Similarly, the energy is the sum of the following terms:

$$e_1(\delta) = \frac{1}{M_0} \int dx u_t'^2(x) = \frac{a}{2} \left[1 - \frac{2a(q+\delta)^2}{1 + e^{a(q+\delta)^2}} \right], \quad (23a)$$

$$e_2(\delta) = \frac{g}{2M_0} \int dx u_t^4(x) \quad (23b)$$

$$= \frac{gM_0\sqrt{a}}{4\sqrt{2\pi}} \frac{(4e^{a(q+\delta)^2/2} + e^{2a(q+\delta)^2} + 3)}{(1 + e^{a(q+\delta)^2})^2},$$

$$e_3(\delta) = \frac{1}{M_0} \int dx V(x) u_t^2(x) \quad (23c)$$

$$= \frac{1}{M_0} \int dx [V_0(x) - g u_0^2(x)] u_t^2(x),$$

where $V_0(x)$ is given by (13b). Again, this last integral must be evaluated numerically. We note in passing that the energy components of Eqs. (23a)-(23c) can be respectively obtained from Eqs. (20a)-(20c) upon setting $\beta = 1$ and replacing $q \mapsto q + \delta$. We plot the energy $e(\delta)$ as a function of δ in Fig. 4 for the case with $a = 1$ and $q = 5$, and for several values of M_0 (again, for both $g = 1$ and $g = -1$). At $\delta = 0$, and for the repulsive case ($g = 1$), the soliton is always stable for all values of M_0 , however for the attractive case ($g = -1$), the soliton again becomes unstable for $M_0 \approx 10$.

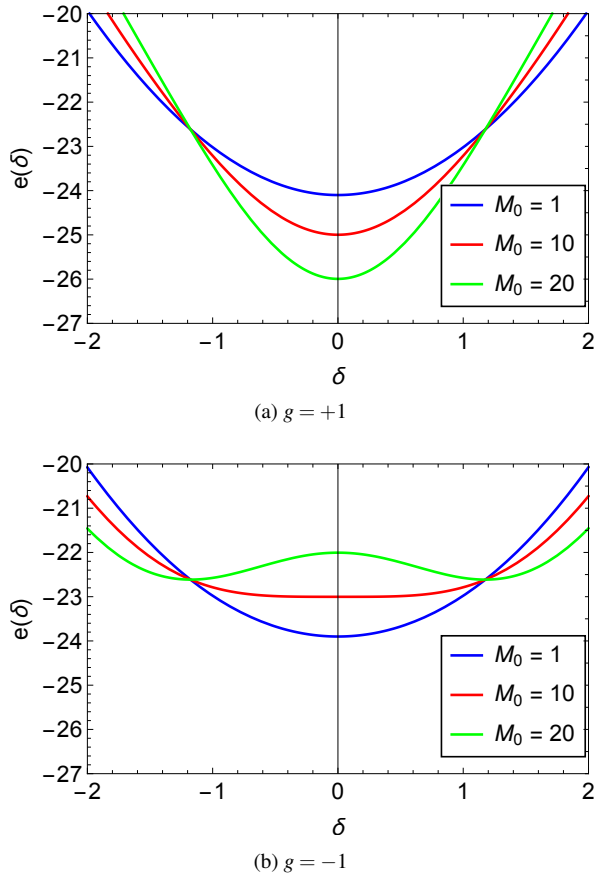


FIG. 4. Same as Fig. 3 but for translational stability. Plots $e(\delta)$ vs. δ for $g = 1$ (top panel) and $g = -1$ (bottom panel) for the cases when $a = 1$ and $q = 5$. Note again that the soliton for $g = 1$ is always stable whereas for $g = -1$, it becomes unstable for $M_0 \approx 10$.

Based on the above two variational studies, we conclude that most likely the two soliton solutions are always stable for repulsive case ($g = 1$) but become unstable for attractive case ($g = -1$). We have also studied a two-soliton wave functions of the form: $u_0(x, y) = A [\text{sech}(q-x) + \text{sech}(q+x)]$, which gives a similar density distribution as the Gaussian case. Numerical results for stretching and translational stability for this ansatz are similar to the Gaussian case discussed above, and indicate stability for the repulsive case and instability for $M \gtrsim 10$ for the attractive case. We will not present those results here.

B. Two dimensions

1. Case 1

We proceed next with the construction of a 2D wave function consisting of two Gaussian functions. In particular, we assume a Gaussian in the x direction centered at $x = \pm q$, and one in the y direction centered at $y = 0$. The ansatz we con-

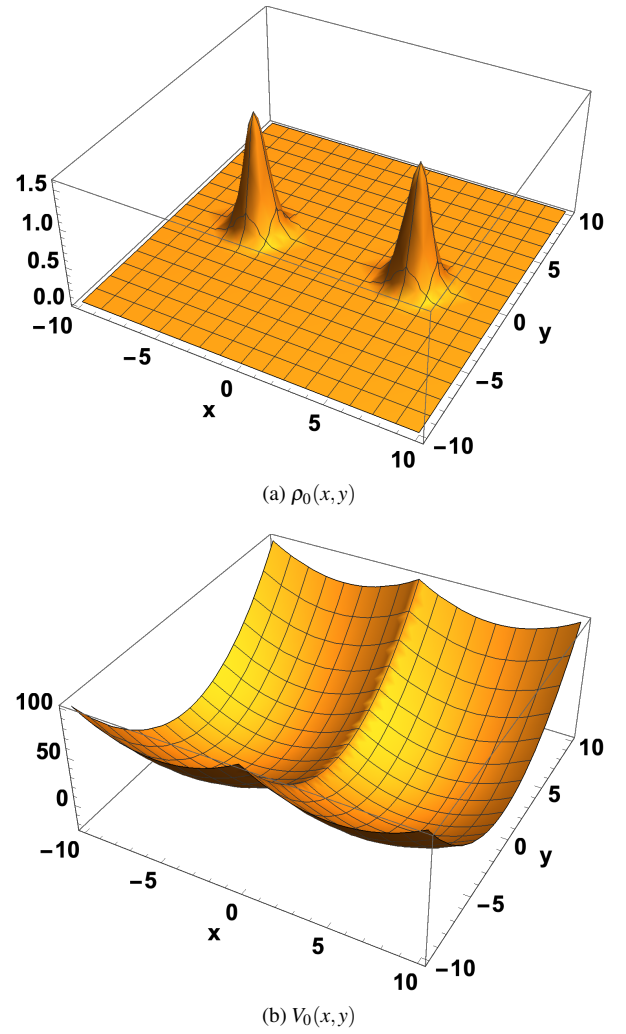


FIG. 5. (a) Plots of the density $\rho_0(x, y)$ and (b) confining potential $V_0(x, y)$ as functions of x and y for the case when $a = b = 1$, $q = 5$, and $M_0 = 10$. The chemical potential is $\mu_0 = b + 2 \text{sech}^2(a) - 1 = 0.000363$.

sider is given explicitly by:

$$u_0(x, y) = A_0 \left\{ e^{-[a(x-q)^2 + by^2]/2} + e^{-[a(x+q)^2 + by^2]/2} \right\} \quad (24)$$

$$= 2A_0 e^{-[a(x^2 + q^2) + by^2]/2} \cosh(aqx).$$

For this case, the conserved mass is given by

$$M_0 = \frac{2\pi}{\sqrt{ab}} (1 + e^{-aq^2}) A_0^2, \quad (25)$$

and the confining potential by:

$$V(x, y) = V_0(x, y) - g u_0^2(x, y), \quad (26a)$$

$$V_0(x, y) = \mu_0 + \{ [\partial_x^2 + \partial_y^2] u_0(x, y) \} / u_0(x, y) \quad (26b)$$

$$= a^2 x^2 + b^2 y^2 - 2a^2 q x \tanh(aqx),$$

where we have chosen $\mu_0 = a + b - (aq)^2$ so that $V_0(0, 0) = 0$. Plots of the density $\rho_0(x, y) = u_0^2(x, y)$ and the potential

$V_0(x, y)$ (both as functions of x and y) for the case when $a = b = 1$, $q = 5$, and $M_0 = 10$ are shown in Fig. 5.

To study stability with respect to a stretching of the coordinates $x \rightarrow \beta x$ and $y \rightarrow \beta y$, we use a trial wave function of the form:

$$u_s(x, y) = 2A_s e^{-[a((\beta x)^2 + q^2) + b(\beta y)^2]/2} \cosh(aq\beta x), \quad (27)$$

where now the mass is given by

$$M_0 = \int d^2x u_s^2(x, y) = \frac{2\pi}{\beta^2 \sqrt{ab}} (1 + e^{-aq^2}) A_s^2. \quad (28)$$

Again computing components of the energy under stretching, we find:

$$e_1(\beta) = \frac{\beta^2}{2} \left[a + b - \frac{2a^2 q^2}{1 + e^{aq^2}} \right], \quad (29a)$$

$$e_2(\beta) = \frac{gM_0 \beta^2 \sqrt{ab}}{16\pi} \frac{(8e^{aq^2/2} + 2e^{2aq^2} + 6)}{(1 + e^{aq^2})^2}, \quad (29b)$$

$$\begin{aligned} e_3(\beta) &= \frac{1}{M_0} \int d^2x V(x, y) u_s^2(x, y) \\ &= \frac{1}{M_0} \int d^2x [V_0(x, y) - g u_0^2(x, y)] u_s^2(x, y), \end{aligned} \quad (29c)$$

where the integral in Eq. (29c) has to be evaluated numerically. The total energy $e(\beta) = e_1(\beta) + e_2(\beta) + e_3(\beta)$ is presented in Fig. 6 as a function of β for $g = \pm 1$ for the case when $a = b = 1$ and $q = 5$, and for various values of the mass M_0 . It can be discerned from the figure that at $\beta = 1$, the soliton for the repulsive case (i.e., $g = 1$) is always stable for all values of M_0 , whereas for the attractive case ($g = -1$), the soliton remains stable for values of $M_0 \lesssim 30$ but becomes unstable for larger values of M_0 .

Translational stability is studied by making the replacement $q \rightarrow q + \delta$, and computing the energy as a function of δ . The trial wave function in this case is given by

$$u_t(x, y) = 2A_t e^{-[a(x^2 + (q+\delta)^2) + by^2]/2} \cosh[a(q + \delta)x], \quad (30)$$

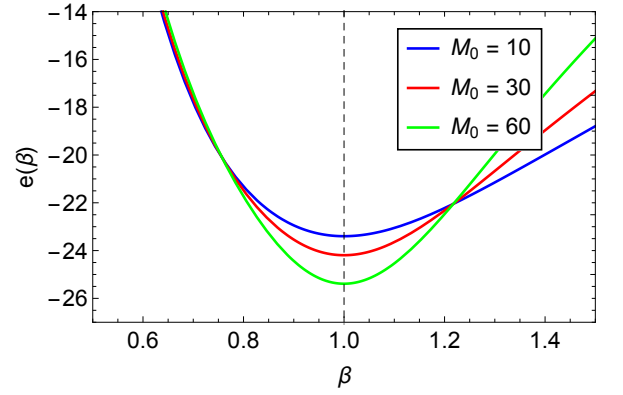
where the total mass reads

$$M_0 = \int d^2x u_t^2(x, y) = \frac{2\pi}{\sqrt{ab}} (1 + e^{-a(q+\delta)^2}) A_t^2. \quad (31)$$

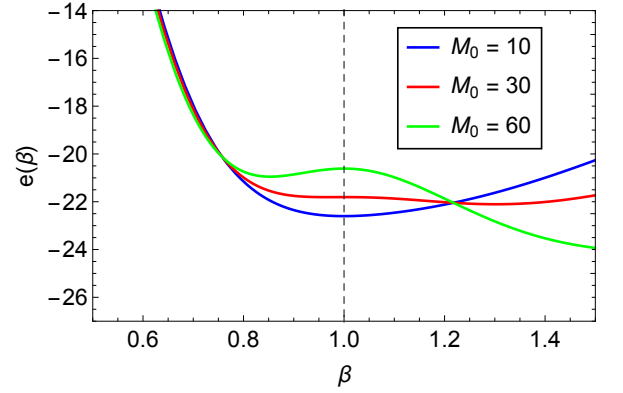
Same as before, the energy terms in this case, i.e., for translational stability are obtained from Eqs. (29) by setting $\beta = 1$ followed by the replacement $q \mapsto q + \delta$. The results for this case are shown in Fig. 7 where the energy $e(\delta)$ is plotted against δ for $g = 1$ and $g = -1$ (see the top and bottom panels, respectively). The soliton solutions for $g = 1$ solitons are always stable whereas the ones with $g = -1$ are stable for values of mass $M_0 \lesssim 30$, and become unstable for larger values of the mass, in agreement with the results of Derrick's theorem in Fig. 6.

2. Case 2

In this case we construct a 2D wave function consisting of two $\text{sech}(x \pm q)$ functions centered at $x = \pm q$, and a Gaussian



(a) $g = +1$



(b) $g = -1$

FIG. 6. Plots of the total energy $e(\beta)$ vs. β for $g = 1$ (top panel) and $g = -1$ (bottom panel), and for case 1 when $a = b = 1$ and $q = 5$.

in the y direction centered at $y = 0$. Explicitly we choose:

$$u_0(x, y) = A_0 [\text{sech}(x + q) + \text{sech}(x - q)] e^{-by^2/2}. \quad (32)$$

For this case, the conserved mass is given by

$$M_0 = 4\sqrt{\frac{\pi}{b}} [1 + q \text{csch}(q) \text{sech}(q)] A_0^2, \quad (33)$$

and the confining potential by:

$$V(x, y) = V_0(x, y) - g u_0^2(x, y), \quad (34a)$$

$$\begin{aligned} V_0(x, y) &= \mu_0 + \{ [\partial_x^2 + \partial_y^2] u_0(x, y) \} / u_0(x, y) \\ &= b^2 y^2 + 2 \text{sech}^2(q) - 2 [\text{sech}^2(q - x) \\ &\quad - \text{sech}(q - x) \text{sech}(q + x) + \text{sech}^2(q + x)], \end{aligned} \quad (34b)$$

where we have chosen $\mu_0 = b + 2 \text{sech}^2(q) - 1$ so that $V_0(0, 0) = 0$. Plots of the density $\rho_0(x, y) = u_0^2(x, y)$ and the potential $V_0(x, y)$ as functions of x and y for the case when $b = 1$, $q = 5$, and $M_0 = 10$ are shown in Fig. 8.

The stability with respect to a stretching of the coordinates $x \rightarrow \beta x$ and $y \rightarrow \beta y$ is carried out by assuming the trial wave function:

$$u_s(x, y) = A_s [\text{sech}(\beta x + q) + \text{sech}(\beta x - q)] e^{-b\beta^2 y^2/2}, \quad (35)$$

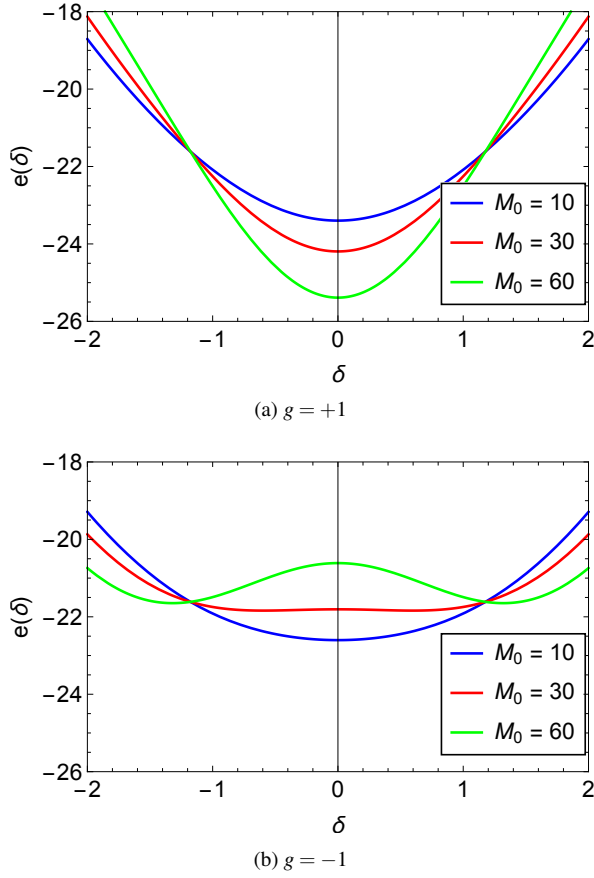


FIG. 7. Same as Fig. 6 but for translational stability. Plots $e(\delta)$ vs. δ for $g = 1$ (top panel) and $g = -1$ (bottom panel) for case 1 when $a = b = 1$ and $q = 5$.

where now the mass is given by

$$M_0 = \frac{4}{\beta^2} \sqrt{\frac{\pi}{b}} [1 + q \operatorname{csch}(q) \operatorname{sech}(q)] A_0^2. \quad (36)$$

Upon computing the energy components in this case we find

$$e_1(\beta) = \frac{\beta^2}{6[1 + q \operatorname{csch}(q) \operatorname{sech}(q)]} \quad (37a)$$

$$\times \left\{ 2 + 3b + 12 \coth(2q) \operatorname{csch}(2q) - 3q[6 + b + (2 - b) \cosh(4q) \operatorname{csch}^3(2q)] \right\},$$

$$e_2(\beta) = \frac{gM\beta^2}{96} \sqrt{\frac{b}{2\pi}} \frac{\operatorname{csch}(q) \operatorname{sech}(q)}{[2q + \sinh(2q)]^2} \quad (37b)$$

$$\times \left\{ -48q + 72q \cosh(2q) - 39 \sinh(2q) + 12 \sinh(4q) + \sinh(6q) \right\},$$

$$e_3(\beta) = \frac{1}{M_0} \int d^2x V(x, y) u_s^2(x, y) \quad (37c)$$

$$= \frac{1}{M_0} \int d^2x [V_0(x, y) - g u_0^2(x, y)] u_s^2(x, y),$$

where the integral in Eq. (37c) has to be evaluated numerically. The total energy $e(\beta) = e_1(\beta) + e_2(\beta) + e_3(\beta)$ is presented in Fig. 9 as a function of β for $g = \pm 1$ for the case

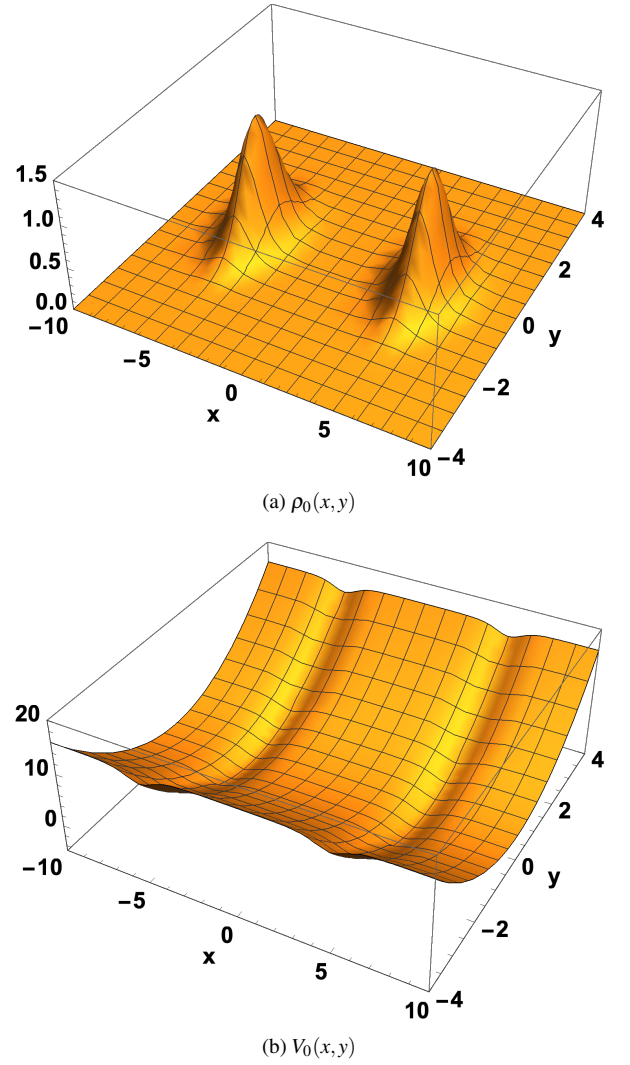


FIG. 8. (a) Plots of the density $\rho_0(x, y)$ and (b) the confining potential $V_0(x, y)$ (again, as functions of x and y) for the case when $b = 1$, $q = 5$, and $M_0 = 10$. The chemical potential is $\mu_0 = b + 2 \operatorname{sech}^2(q) - 1 = 0.000363$.

when $a = b = 1$ and $q = 5$, and for various values of the mass M_0 . It can be discerned from the figure that at $\beta = 1$, the soliton for the repulsive case (i.e., $g = 1$) is always stable for all values of M_0 , whereas for the attractive case ($g = -1$), the soliton remains stable for values of $M_0 \lesssim 20$ but becomes unstable for larger values of M_0 .

Translational stability is studied by making the replacement $q \rightarrow q + \delta$, and computing the energy as a function of δ . The trial wave function in this case is given by

$$u_t(x, y) = A_t [\operatorname{sech}(x + q + \delta) + \operatorname{sech}(x - q - \delta)] e^{-by^2/2}, \quad (38)$$

where the total mass is now given by

$$M_0 = 4 \sqrt{\frac{\pi}{b}} [1 + (q + \delta) \operatorname{csch}(q + \delta) \operatorname{sech}(q + \delta)] A_t^2. \quad (39)$$

Again, the energy terms for translational instability are ob-

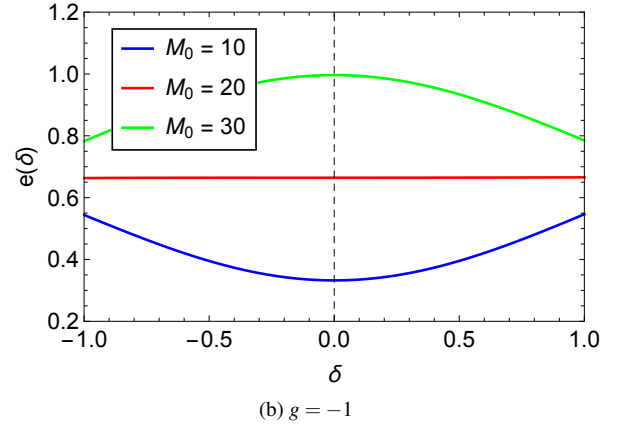
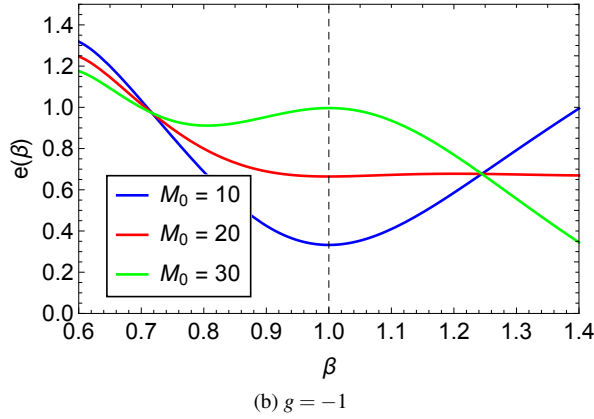
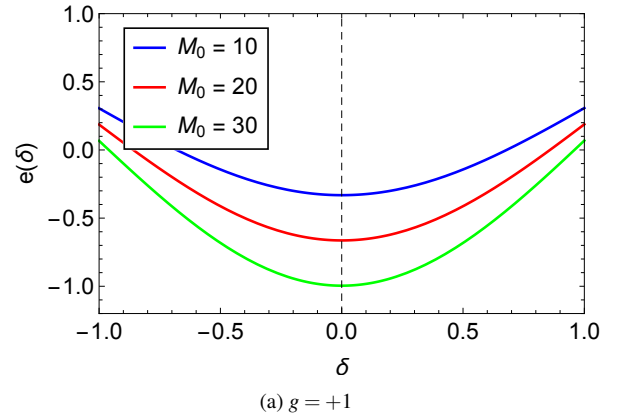
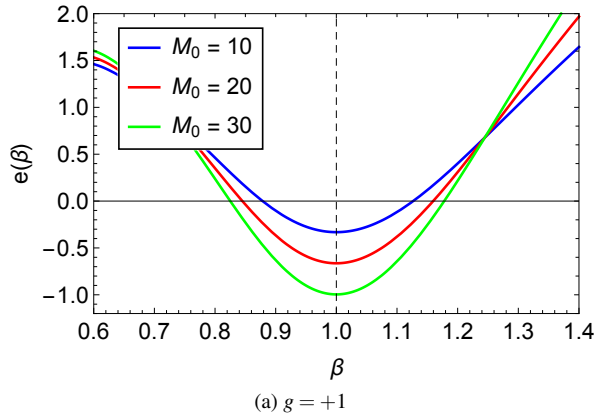


FIG. 9. Plots of the total energy $e(\beta)$ vs. β for $g = 1$ (top panel) and $g = -1$ (bottom panel), and for case 2 when $b = 1$ and $q = 5$.

FIG. 10. Same as Fig. 9 but for translational stability. Plots of $e(\delta)$ vs. δ for $g = 1$ (top panel) and $g = -1$ (bottom panel) for the case 2 when $b = 1$ and $q = 5$.

tained from the expressions (37) by setting initially $\beta = 1$, and making the replacement $q \rightarrow q + \delta$ afterwards. The results in this case for the energy $e(\delta)$ as a function of δ are shown in Fig. 10. The $g = 1$ solitons are always stable whereas the $g = -1$ solitons are stable for values of mass $M_0 \lesssim 20$, and become unstable for larger values of the mass, in agreement with the results of Derrick's theorem in Fig. 9.

C. Three dimensions

Two spheroidal BEC solitons have been studied for a variety of reasons in the literature, the most intriguing being to determine whether modifications of quantum mechanics due to general relativity can be seen in this type of system. In most of these problems an approximate confining potential is used so that questions of stability of the BEC as one increases the number of atoms can be addressed. Indeed, we can first reverse engineer the exact potential needed to make the sum of two Gaussians an exact solution. Then, we can determine the stability criteria for soliton solutions using Derrick's theorem as well as linear response theory.

1. Two solitons

We start by constructing a 3D Gaussian, two-soliton solution of the form:

$$u_0(x, y, z) = A_0 e^{-a(x^2+y^2)/2} \left[e^{-b(q+z)^2/2} + e^{-b(q-z)^2/2} \right] \quad (40)$$

$$= 2A_0 e^{-[a(x^2+y^2)+b(z^2+q^2)]/2} \cosh(bqz).$$

Here we chose the center of the soliton at $x = y = 0$ and $z = \pm q$ for simplicity. The mass is now given by:

$$M_0 = \frac{2\pi^{3/2}}{a\sqrt{b}} (1 + e^{-bq^2}) A_0^2, \quad (41)$$

and the confining potential by:

$$V(x, y, z) = V_0(x, y, z) - g u_0^2(x, y, z), \quad (42)$$

$$V_0(x, y, z) = a^2(x^2 + y^2) + b^2 z^2 - 2b^2 qz \tanh(bqz),$$

where we have chosen $\mu_0 = b + 2a - b^2 q^2$ so that $V_0(0, 0, 0) = 0$. Plots of the density $\rho_0(x, y, z)$ and potential $V_0(x, y, z)$ as functions of x , y , and z , are shown in Fig. 11.

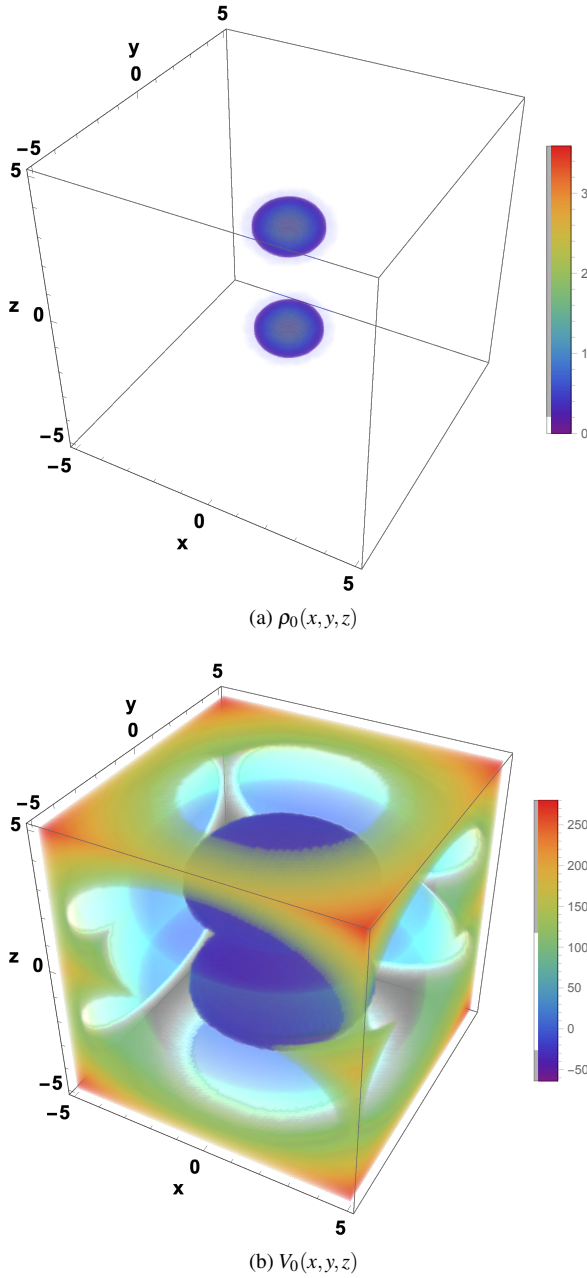


FIG. 11. (a) Plots of the density $\rho_0(x,y,z)$ and (b) the confining potential $V_0(x,y,z)$ (both as functions of x, y , and z) for the case when $a = 2, b = 4, q = 2$, and $M_0 = 10$. The chemical potential is $\mu_0 = b + 2a - (bq)^2 = -56$.

2. Three solitons

There are many possibilities for obtaining N -soliton solutions in 3D. The simplest three soliton case is given by

$$u_0(x,y,z) = A_0 e^{-[a(x^2+y^2)/2+bz^2]/2} H_n(\sqrt{b}z), \quad (43)$$

where $H_n(\zeta)$ is a Hermite polynomial of order n . In this case, the conserved mass is given by

$$M_0 = \frac{\pi^{3/2} 2^2 n!}{a\sqrt{b}} A_0^2, \quad (44)$$

and the confining potential by

$$V(x,y,z) = V_0(x,y,z) - g u_0^2(x,y,z), \quad (45)$$

$$V_0(x,y,z) = 2bn + a^2(x^2 + y^2) + b^2 z^2 - \frac{4b^{3/2} n z H_{n-1}(\sqrt{b}z) - 4bn(n-1) H_{n-2}(\sqrt{b}z)}{H_n(\sqrt{b}z)},$$

where we have chosen $\mu_0 = 2a + (2n + 1)b$ so that $V_0(0,0,0) = 0$. Plots of the density $\rho_0(x,y,z)$ and potential $V_0(x,y,z)$ (both as functions of x, y , and z) are shown in Fig. 12 for the three soliton case with parameter values $n = 2, a = 1, b = 2$, and $M_0 = 10$.

One can analytically determine the energy of the stretched soliton in this case with $x_i \rightarrow \beta x_i$ ($i = 1, 2, 3$) keeping the mass M fixed. The total energy in this case is:

$$e(\beta) = e_1(\beta) + e_2(\beta) + e_3(\beta), \quad (46)$$

with

$$e_1(\beta) = \frac{1}{2} \beta^2 (2a + 5b), \quad (47a)$$

$$e_2(\beta) = \frac{41a\sqrt{b}\beta^3 gM}{256\sqrt{2}\pi^{3/2}}, \quad (47b)$$

$$e_3(\beta) = \frac{2a + 5b}{2\beta^2} - \frac{a\sqrt{b} (2\beta^8 - 16\beta^6 + 69\beta^4 - 16\beta^2 - 2) \beta^3 gM}{4\pi^{3/2} (\beta^2 + 1)^{11/2}}.$$

One easily verifies that $\beta = 1$ is a stationary point. Setting the second derivative to zero at $\beta = 1$ gives the criterion for instability of the $g < 0$ soliton to set in, that is

$$M_c = -g \frac{2048\sqrt{2}\pi^{3/2}(2a + 5b)}{1527a\sqrt{b}}. \quad (48)$$

For $g = -1, a = 2, b = 2$ we find $M_c = 89.62$.

IV. LINEAR RESPONSE EQUATIONS

Solutions of the linear response equations (8) are obtained by consideration of an eigenvalue equation. Let the pair $(a(\mathbf{r}), b(\mathbf{r})) \in \mathbb{C}^2$ satisfy the skew-symmetric eigenvalue equation:

$$\begin{pmatrix} [h(\mathbf{r}) + g u_0^2(\mathbf{r})] & g u_0^2(\mathbf{r}) \\ -g u_0^2(\mathbf{r}) & -[h(\mathbf{r}) + g u_0^2(\mathbf{r})] \end{pmatrix} \begin{pmatrix} a(\mathbf{r}) \\ b(\mathbf{r}) \end{pmatrix} = \mu \begin{pmatrix} a(\mathbf{r}) \\ b(\mathbf{r}) \end{pmatrix}, \quad (49)$$

where $\mu \in \mathbb{C}$ is the eigenvalue. Here $h(\mathbf{r})$ is given by (9)

$$h(\mathbf{r}) = -\nabla^2 + V_0(\mathbf{r}), \quad (50)$$

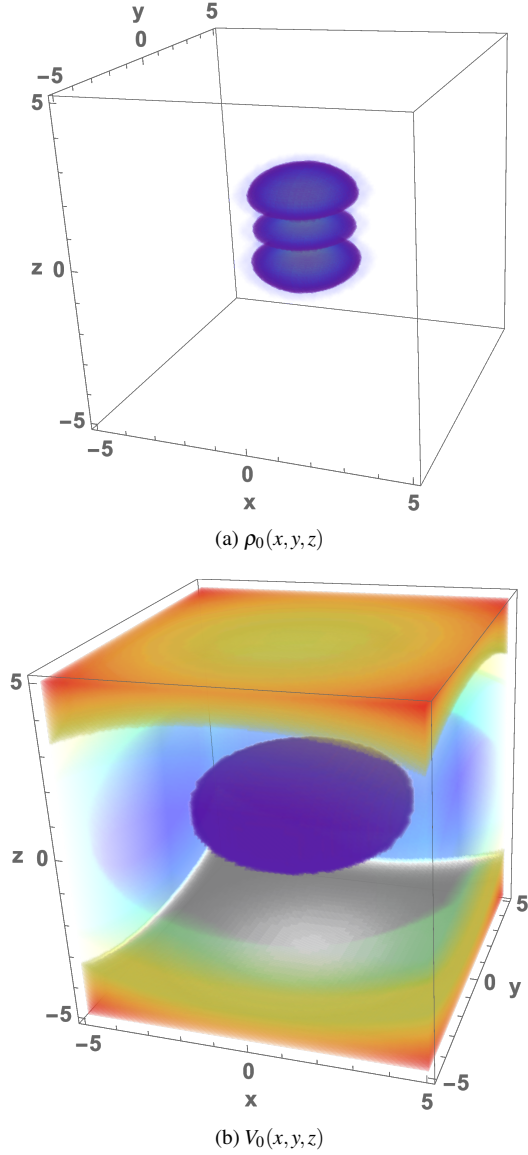


FIG. 12. (a) Plots of the density $\rho_0(x, y, z)$ and (b) the confining potential $V_0(x, y, z)$ (both as functions of x , y , and z) for the three-soliton Hermite case when $n = 2$, $a = 1$, $b = 2$, and $M_0 = 10$. The chemical potential is $\mu_0 = 2a + 5b = 12$.

and is *independent* of the mass M_0 . Equations (49) are sometimes called the Bogoliubov-de Gennes (BdG) equations^{20,21}.

By taking the complex conjugate of (49), interchanging top and bottom lines, and multiplying by -1 , we see that if $(a(\mathbf{r}), b(\mathbf{r}))$ are a pair of solutions with eigenvalue μ , then $(b^*(\mathbf{r}), a^*(\mathbf{r}))$ are a pair of solutions of (49) with eigenvalue $-\mu^*$. In other words, the eigenvalues come as pairs, μ and $-\mu^*$. Multiplying the bottom line of (49) by -1 and making use of the Hermitian property of the operator on the left-hand-side yields an orthogonality relation:

$$(\mu_i^* - \mu_j) \int d^3x [a_i^*(\mathbf{r})a_j(\mathbf{r}) - b_i^*(\mathbf{r})b_j(\mathbf{r})] = 0. \quad (51)$$

Real eigenvalues lead to oscillatory behavior and stability

whereas imaginary eigenvalues lead to blow up or damping and instability of the system. The system is deemed stable if $\text{Im}\{\mu_i\} = 0$ for all i . For real eigenvalues, the states are normalized by:

$$\int d^3x [a_i^*(\mathbf{r})a_j(\mathbf{r}) - b_i^*(\mathbf{r})b_j(\mathbf{r})] = \delta_{i,j}. \quad (52)$$

The general solution to (8) is then given by the sum over all eigenstates of (49):

$$\begin{aligned} \Phi(\mathbf{r}, t) &= \begin{pmatrix} \phi(\mathbf{r}, t) \\ \phi^*(\mathbf{r}, t) \end{pmatrix} = \sum_{\text{all } i} \Phi_i \begin{pmatrix} c_i(\mathbf{r}) \\ d_i^*(\mathbf{r}) \end{pmatrix} e^{-i\mu_i t} \\ &= \sum_{i>0} \Phi_i \left\{ \begin{pmatrix} a_i(\mathbf{r}) \\ b_i(\mathbf{r}) \end{pmatrix} e^{-i\mu_i t} + \begin{pmatrix} b_i^*(\mathbf{r}) \\ a_i^*(\mathbf{r}) \end{pmatrix} e^{+i\mu_i^* t} \right\}, \end{aligned} \quad (53)$$

the last sum now going over the unique eigenvalues only. At $t = 0$,

$$\begin{pmatrix} \phi(\mathbf{r}, 0) \\ \phi^*(\mathbf{r}, 0) \end{pmatrix} = \sum_i \Phi_i \begin{pmatrix} c_i(\mathbf{r}) \\ d_i^*(\mathbf{r}) \end{pmatrix}. \quad (54)$$

Inverting this relation using (52)

$$\begin{aligned} \int d^3x (c_j^*(\mathbf{r}), d_j(\mathbf{r})) \begin{pmatrix} 1 & 0 \\ 0 & -1 \end{pmatrix} \begin{pmatrix} \phi(\mathbf{r}, 0) \\ \phi^*(\mathbf{r}, 0) \end{pmatrix} \\ = \sum_i \Phi_i (c_j^*(\mathbf{r}), d_j(\mathbf{r})) \begin{pmatrix} 1 & 0 \\ 0 & -1 \end{pmatrix} \begin{pmatrix} c_i(\mathbf{r}) \\ d_i^*(\mathbf{r}) \end{pmatrix} = \Phi_j, \end{aligned} \quad (55)$$

gives

$$\Phi_i = \int d^3x [c_i^*(\mathbf{r})\phi(\mathbf{r}, 0) - d_i(\mathbf{r})\phi^*(\mathbf{r}, 0)]. \quad (56)$$

Solutions of the NLSE to first order are then given by

$$\Psi(\mathbf{r}, t) = \Psi_0(\mathbf{r}, t) + \varepsilon \Phi(\mathbf{r}, t) + \dots \quad (57)$$

where

$$\Psi_0(\mathbf{r}, t) = \begin{pmatrix} u_0(\mathbf{r}) e^{-i\mu_0 t} \\ u_0(\mathbf{r}) e^{+i\mu_0 t} \end{pmatrix}. \quad (58)$$

We must also require that

$$\Psi_0^\dagger(\mathbf{r}, t) M \Phi(\mathbf{r}, t) = 0, \quad M = \begin{pmatrix} 1 & 0 \\ 0 & -1 \end{pmatrix}, \quad (59)$$

since the unperturbed state is included in $\Psi_0(\mathbf{r}, t)$. This requirement is usually applied by omitting the $i = 0$ state in the sum appearing in Eq. (53), as discussed in the next section.

A. One dimension

In 1D, the eigenvalue equation (49) becomes:

$$\begin{pmatrix} [h(x) + gu_0^2(x)] & gu_0^2(x) \\ -gu_0^2(x) & -[h(x) + gu_0^2(x)] \end{pmatrix} \begin{pmatrix} a(x) \\ b(x) \end{pmatrix} = \lambda \begin{pmatrix} a(x) \\ b(x) \end{pmatrix}, \quad (60)$$

where $u_0(x)$ is given by Eq. (11), and

$$h(x) = -\partial_x^2 + V_0(x), \quad (61)$$

$$V_0(x) = -a(1 - aq^2) + a^2x(x - 2q \tanh(aqx)). \quad (62)$$

Here we have set $\mu = \mu_0 + \lambda$, and redefined $V_0(x)$ so that now $V_0(0) = \mu_0 = a(1 - aq^2)$. A plot of this potential as a function of x is shown in Fig. 13(a) for the case when $a = 1$ and $q = 5$. Zero eigenvalues ($\lambda = 0$) now correspond to the soliton solution $a(x) = -b(x) = u_0(x)$.

1. Bogoliubov approximation

Moreover, the eigenvalue problem (60) can be written in terms of eigenvectors of the Hermitian operator $h(x)$ in 1D. To that effect, we define

$$h(x) \chi_n(x) = \varepsilon_n \chi_n(x), \quad \chi_n(x) \in \mathbb{R}, \quad (63)$$

where $\varepsilon_n \in \mathbb{R}$ and $\chi_n(x)$ obeys the orthonormal relation,

$$\int dx \chi_n(x) \chi_{n'}(x) = \begin{cases} \delta_{n,n'}, & \text{for } n \text{ and } n' \neq 0, \\ M_0, & \text{for } n = n' = 0. \end{cases} \quad (64)$$

For our case when $a = 1$ and $q = 5$, the eigenvalues are very close to being doubly degenerate and are given by $\varepsilon_n = 0, 2, 4, 6, \dots$ with a small splitting of each state due to tunneling between the two wells. The low lying spectrum is that of a quantum harmonic oscillator with frequency $\omega = 2$, as might be expected from the shape of the double well. A plot of the first few wave functions $\chi_n(x)$ (as functions of x) are shown in Fig. 13(b).

Expanding the solutions of (60) by setting

$$\begin{pmatrix} a(x) \\ b(x) \end{pmatrix} = \sum_{n=0}^{\infty} \begin{pmatrix} A_n(x) \\ B_n(x) \end{pmatrix} \chi_n(x), \quad (65)$$

and using the orthonormal condition, we obtain the eigenvalue problem

$$\sum_{n'=0}^{\infty} \begin{pmatrix} (\varepsilon_n - \lambda) \delta_{n,n'} + g \Delta_{n,n'} & g \Delta_{n,n'} \\ -g \Delta_{n,n'} & -(\varepsilon_n + \lambda) \delta_{n,n'} - g \Delta_{n,n'} \end{pmatrix} \times \begin{pmatrix} A_{n'}(x) \\ B_{n'}(x) \end{pmatrix} = 0, \quad (66)$$

where

$$\Delta_{n,n'} = \int dx u_0^2(x) u_n(x) u_{n'}(x). \quad (67)$$

The eigenvalues λ are then found by solving the determinant:

$$\begin{vmatrix} (\varepsilon_n - \lambda) \delta_{n,n'} + g \Delta_{n,n'} & g \Delta_{n,n'} \\ -g \Delta_{n,n'} & -(\varepsilon_n + \lambda) \delta_{n,n'} - g \Delta_{n,n'} \end{vmatrix} = 0. \quad (68)$$

Numerical calculations for the case when $a = 1$ and $q = 5$ gives $\Delta_{1,1} \approx 0.2M_0$ and $\Delta_{2,2} \approx 0.1M_0$, whereas $\Delta_{1,2} =$

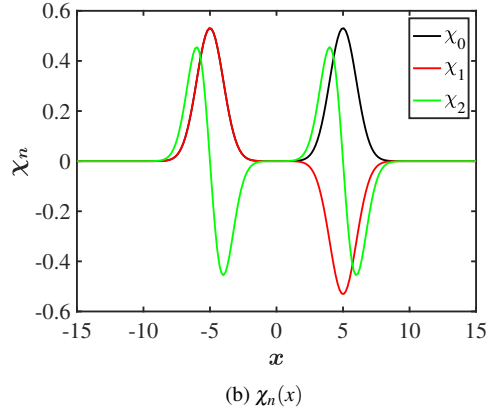
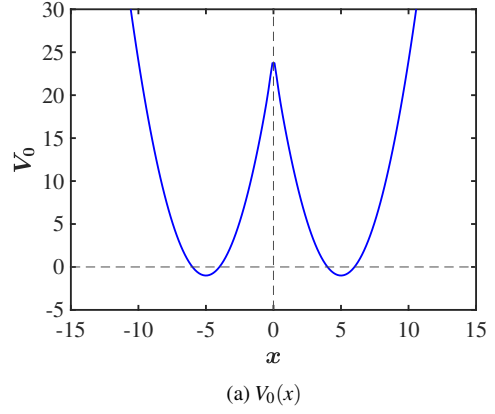


FIG. 13. (a) Plots of the potential $V_0(x)$ in Eq. (62) and (b) the wave functions $\chi_n(x)$ in Eq. (64) as functions of x for the case when $a = 1$ and $q = 5$.

$10^{-9}M_0$ and $\Delta_{0,3} = -0.705M_0$. So a reasonable approximation for the low-lying eigenvalues is to include only diagonal terms, $\Delta_{n,n'} \approx \Delta_n \delta_{n,n'}$, in which case (68) becomes

$$\begin{vmatrix} \varepsilon_n - \lambda + g \Delta_n & g \Delta_n \\ -g \Delta_n & -\varepsilon_n - \lambda - g \Delta_n \end{vmatrix} = 0, \quad (69)$$

which gives

$$\lambda_n = \pm \sqrt{\varepsilon_n(\varepsilon_n + 2g\Delta_n)}, \quad (70)$$

which is the Bogoliubov spectrum. One can see here that for $g = +1$ the system is always stable whereas for $g = -1$ there is a small region of stability as long as

$$\varepsilon_n \geq 2g\Delta_n, \quad (71)$$

for any n . For $n = 1$ in our case this means that $2 > 0.4M_0$, or $M_0 < 5$. For $n = 2$, we find $M_0 < 20$, which is a higher bound.

2. Direct solution of the BdG equation

The eigenvalue equation of Eq. (60) is solved numerically in MATLAB by employing a computational grid in coordinate space, and using a fourth-order accurate, finite difference

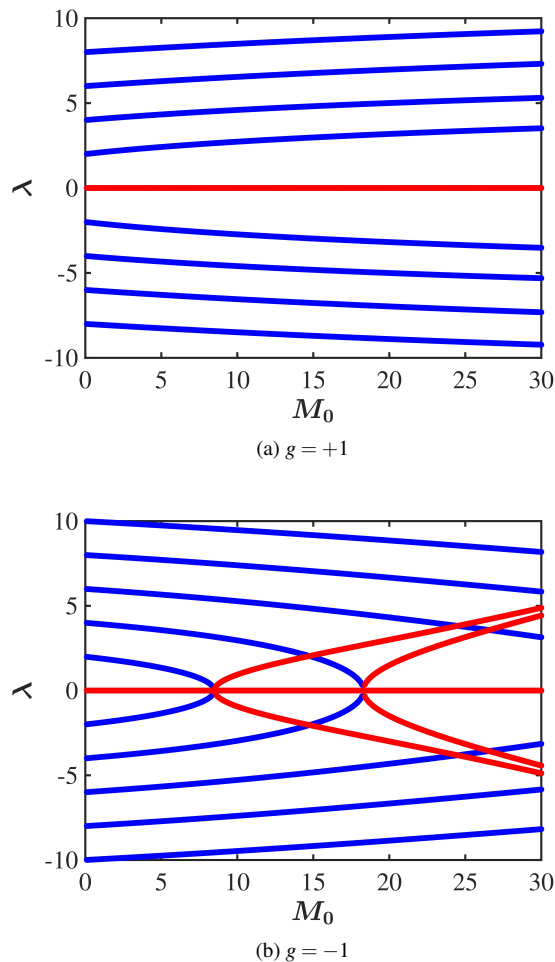


FIG. 14. Real (blue lines) and imaginary (red lines) parts of the eigenvalues λ in Eq. (60) as functions of M_0 for the one-dimensional case with $a = 1$ and $q = 5$.

approximation for the Laplacian operator. We corroborated our numerical results by using P_3 finite elements in the computational software FreeFEM++²⁴ that utilizes the ARPACK eigenvalue solver²⁵, and obtained similar results.

In 1D, numerical results for the eigenvalues λ of this calculation are plotted in Fig. 14 as functions of M_0 for $g = \pm 1$ and parameter values $a = 1$ and $q = 5$. The real part of the eigenvalues is shown in red whereas their imaginary part is shown in blue. The top panel of the figure corresponding to the repulsive ($g = 1$) case suggests that the solution is linearly stable. On the other hand, when we consider attractive interactions, i.e., $g = -1$, the solution is (linearly) stable but becomes unstable past $M_0 \gtrsim 8$, in approximate agreement with the Bogoliubov approximation and Derrick’s theorem (see Section III A). At $M_0 = 0$, the low-lying eigenvalues are all real and given by $\lambda_n \approx 0, 2, 4, 6, \dots$. Moreover, we compare the (1D) numerical results of Eq. (60) for $g = -1$ (see, the bottom panel of Fig. 14) with the approximate Bogoliubov result from Eq. (70) in Fig. 15. The shape of the Bogoliubov curve shown with dashed black line is proximal

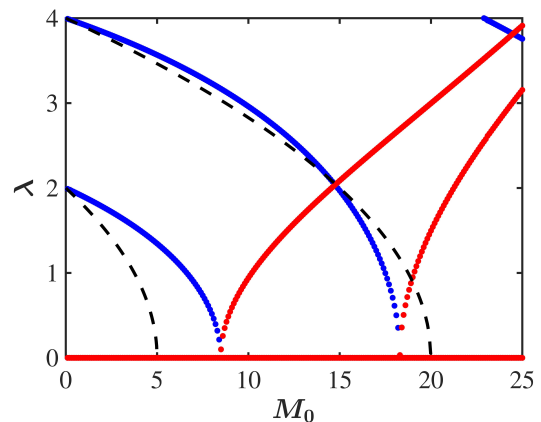


FIG. 15. Comparison of the real part of the $g = -1$ numerically (exact) eigenvalues λ (in blue) with the Bogoliubov formula (in dashed black) of Eq. (70).

to the numerically computed eigenvalues although the point in the parameter space where the solution is predicted to be unstable is at lower values of M_0 . This is somewhat expected because not enough terms were included in Eq. (68) which itself would allow otherwise a better agreement between the two approaches.

Similar conclusions are drawn in the 2D case (see, Sec. III B). To that end, we briefly discuss our findings in Fig. 16 which depicts numerical results for the eigenvalues λ (see, also Sec. III B) when $a = b = 1$ and $q = 5$. Again the system is stable when $g = -1$ for all values of M_0 , whereas when $g = +1$ there is a region of stability for $M_0 \lesssim 7.5$. We note in passing that we have checked the stability and instability (over the respective parameter regime) of the solutions that we have presented so far by performing direct numerical simulations of the GPE [cf. Eq. (1)] although we omit the presentation of the respective results herein.

V. CONCLUSIONS

In this paper, we considered the nonlinear Schrödinger equation (NLSE) or Gross-Pitaevskii equation (GPE), and employed the “inverse problem” method for the potential therein. We discussed various such external potentials in 1D and higher spatial dimensions, and obtained respective exact yet confined solutions. We showed that these solutions to the NLSE may possess an arbitrary number of “soliton-like” maxima, i.e., N -soliton solutions. Since these solutions are exact, we can obtain analytical estimates for the values of the L^2 norm of the solution or, equivalently, the number of atoms in the trap above which these solutions are unstable to width perturbations using Derrick’s theorem. We further solved numerically the underlying eigenvalue (BdG) problem emanating from the linearization of the NLSE whose results are in line (in terms of stability characteristics) with the theoretical predictions from Derrick’s theorem. However, in all cases that we have studied in this work that turned out to be

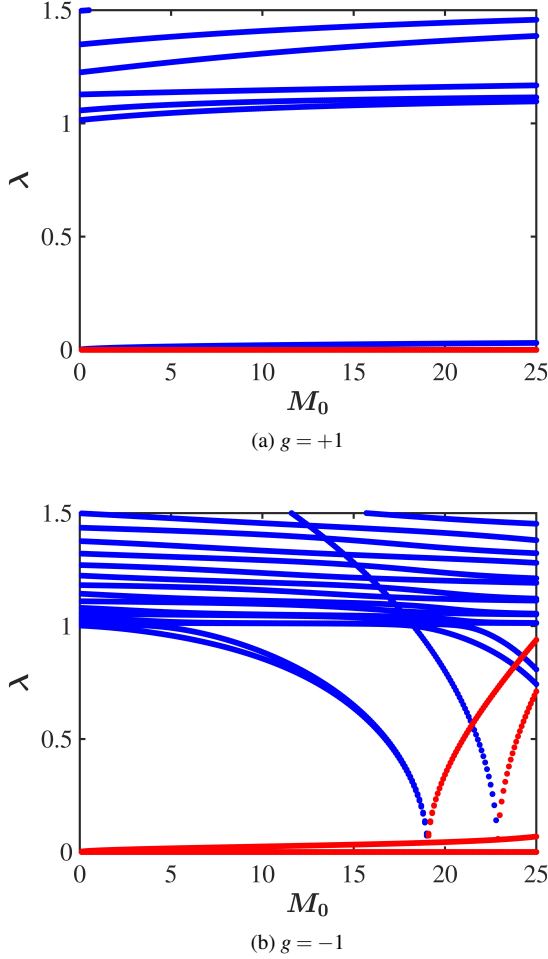


FIG. 16. The real part (in blue) and imaginary part (in red) of the eigenvalues for the two-dimensional soliton of Eq. (32) as functions of M_0 for the $g = \pm 1$ cases, with $a = b = 1$ and $q = 5$.

unstable (i.e., attractive interactions), the BdG analysis gives a lower value for the critical value of the norm of the wave function than Derrick's theorem or the translational instability. To the extent that we can identify these distinct entities as separate BEC solutions of the Gross-Pitaevskii equation, then we have given a prescription for what external potentials will produce various configurations of BECs that are stable in 1D and higher spatial dimensions.

Appendix A: Some other N -soliton solutions in 2D

It is clear that there are infinite possibilities for exact N -soliton solutions in 2D and 3D. Here we will give two examples not included in the main text. For the sum of Gaussians, it is easy to generalize to N soliton exact solutions. As an example of this, consider the case where the solitons are centered at the ends of an equilateral triangle. That is, we take for the

initial condition:

$$u(x, y) = A \left\{ e^{-a(y-\sqrt{3}q)^2/2 - ax^2/2} + e^{-ay^2/2} \left[e^{-a(x-q)^2/2} + e^{-a(q+x)^2/2} \right] \right\}, \quad (\text{A1})$$

and obtain from the inverse method:

$$\mu_0 = 2a - a^2 q^2 - \frac{a^2 q^2}{e^{aq^2} + 1/2}, \quad (\text{A2})$$

together with $V(x, y) = V_1(x, y) + V_2(x, y)$ where

$$V_1(x, y) = -A^2 g e^{-a(3q^2 + 2qx + x^2 + y^2)} \times \left[e^{aq^2} + e^{aq(x+\sqrt{3}y)} + e^{aq(q+2x)} \right]^2 \quad (\text{A3})$$

and

$$V_2(x, y) = \frac{a^2}{(2e^{aq^2} + 1)(e^{aq^2} + e^{aq(x+\sqrt{3}y)} + e^{aq(q+2x)})} \times \left\{ e^{aq(q+2x)}(-2q^2 - 2qx + x^2 + y^2) + 2e^{2aq^2}(2qx + x^2 + y^2) + e^{aq^2}(-2q^2 + 2qx + x^2 + y^2) + 2(2q^2 - 2\sqrt{3}qy + x^2 + y^2)e^{aq(q+x+\sqrt{3}y)} + 2e^{2aq(q+x)}(-2qx + x^2 + y^2) + (-2\sqrt{3}qy + x^2 + y^2)e^{aq(x+\sqrt{3}y)} \right\}. \quad (\text{A4})$$

For the choice of parameters values $g = -1, A = 1, a = 1$, and $q = 3$, we depict the density $\rho(x, y)$ and potential $V(x, y)$ in Fig. 17. One can also have solitons along both the x - and y -axes by choosing

$$u_0(x, y) = AH_n(\sqrt{ax})H_m(\sqrt{by})e^{-ax^2/2 - by^2/2}, \quad (\text{A5})$$

for which one has $n + 1$ solitons in x -direction and $m + 1$ solitons in y -direction where

$$V(x, y) = a^2 x^2 + b^2 y^2 - gA^2 H_n^2(\sqrt{ax})H_m^2(\sqrt{by})e^{-ax^2/2 - by^2/2}, \quad (\text{A6})$$

with $\mu_0 = (2n + 1)a + (2m + 1)b$. When $m = n = 2$, the trapped solution has 9 peaks. For that case we obtain

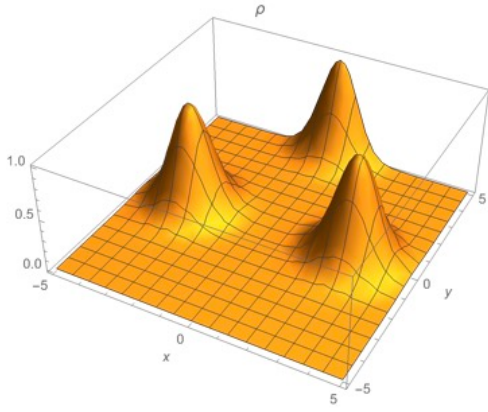
$$M_0 = 64\pi A^2 / \sqrt{ab}, \quad (\text{A7a})$$

$$\rho(x, y) = A^2(2 - 4ax^2)^2(2 - 4by^2)^2 e^{-ax^2 - by^2}, \quad (\text{A7b})$$

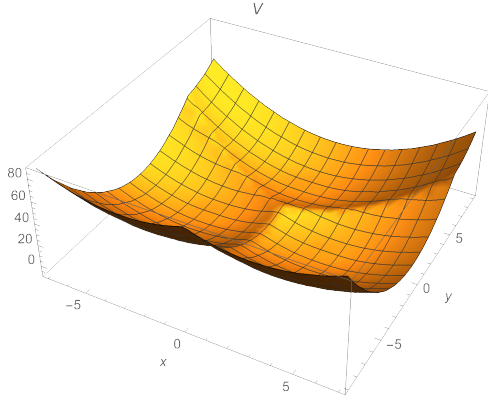
$$V(x, y) = a^2 x^2 + b^2 y^2 - 16A^2 g(1 - 2ax^2)^2(1 - 2by^2)^2 e^{-ax^2 - by^2}, \quad (\text{A7c})$$

and with $\mu_0 = 5(a + b)$. An example of this for $m = n = 2$ and $A = 1, a = 1, b = 2$, and with $g = -1$ is shown in Figs 18. Derrick's theorem in this case allows us to determine the critical mass for instability, which is given by:

$$M_c = \frac{81920\pi(a+b)}{11029\sqrt{ab}}. \quad (\text{A8})$$



(a)Density



(b)Confining potential

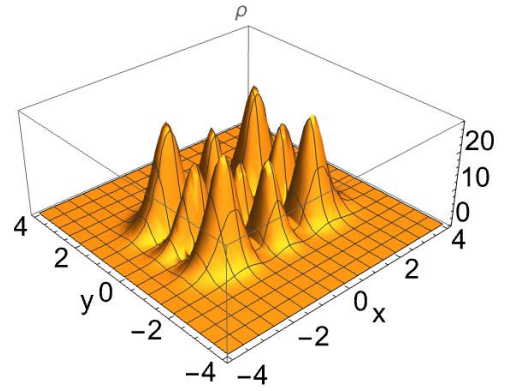
FIG. 17. The density $\rho(x,y)$ and the confining potential $V(x,y)$ both as functions of x and y for the three soliton case, when $g = -1, a = 1, q = 3$, and $A = 1$.

For $a = 1, b = 2$, and $g = -1$ we find:

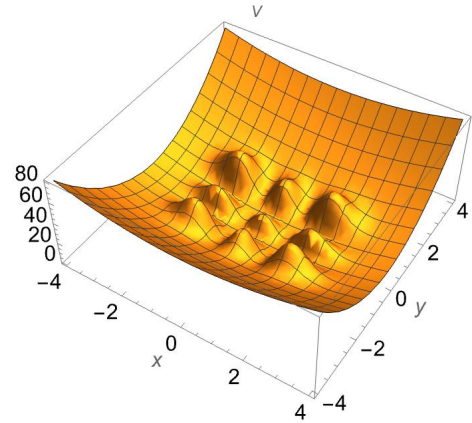
$$M_c = \frac{122880\sqrt{2}\pi}{11029} \approx 49.5. \quad (\text{A9})$$

ACKNOWLEDGMENTS

The motivation for working on this problem resulted from discussions that one of us (FC) had with Alan Chodos on using BECs to test modifications of gravity. FC, JFD, and EGC would like to thank the Santa Fe Institute and the Center for Nonlinear Studies at Los Alamos National Laboratory for their kind hospitality. One of us (AK) is grateful to Indian National Science Academy (INSA) for the award of INSA Honorary Scientist position at Savitribai Phule Pune University. The work of EGC has been supported by the U.S. National Science Foundation under Grants No. DMS-2204782. The work at Los Alamos National Laboratory was carried out under the auspices of the U.S. DOE and NNSA under Contract No. DEAC52-06NA25396.



(a)Density



(b)Confining potential

FIG. 18. The density $\rho(x,y)$ and the confining potential $V(x,y)$ both as functions of x and y , for the nine soliton case, when $m = n = 2, g = -1, A = 1, a = 1$, and $b = 2$.

- ¹M. J. Ablowitz, B. Prinari, and A. Trubatch, *Discrete and Continuous Nonlinear Schrödinger Systems*, Vol. 302 (Cambridge University Press, Cambridge, 2004).
- ²A. Hasegawa and K. Kodama, *Solitons in Optical Communications* (Clarendon Press, 1995).
- ³Y. Kivshar and G. Agrawal, *Optical Solitons: From Fibers to Photonic Crystals* (Academic Press, USA, 2003).
- ⁴V. Zakharov, "Stability of periodic waves of finite amplitude on the surface of a deep fluid," *J. Appl. Mech. Tech. Phys.* **9**, 190–194 (1968).
- ⁵M. J. Ablowitz, *Nonlinear Dispersive Waves: Asymptotic Analysis and Solitons* (Cambridge University Press, Cambridge, 2011).
- ⁶M. Kono and M. Skorić, *Nonlinear Physics of Plasmas* (Springer-Verlag, Heidelberg, 2010).
- ⁷E. P. Gross, "Structure of a quantized vortex in boson systems," *Il Nuovo Cimento (1955-1965)* **20**, 454–477 (1961).
- ⁸L. P. Pitaevskii, "Vortex lines in an imperfect Bose gas," *Soviet Phys. JETP* **20**, 451 (1961).
- ⁹L. Pitaevskii and S. Stringari, *Bose-Einstein Condensation and Superfluidity* (Oxford University Press, Oxford, 2015).
- ¹⁰S. Cornish, N. Claussen, J. Roberts, E. Cornell, and C. Wieman, *Phys. Rev. Lett.* **85**, 1795 (2000).
- ¹¹K. Strecker, G. Partridge, A. Truscott, and R. Hulet, *Nature* **417**, 150 (2001).
- ¹²L. Landau and E. Lifshitz, *Quantum Mechanics: Non-Relativistic Theory*, Vol. 3 (Butterworth-Heinemann, Boston, 2003).

- ¹³E. G. Charalampidis, P. G. Kevrekidis, D. J. Frantzeskakis, and B. A. Malomed, “Dark-bright solitons in coupled nonlinear Schrödinger equations with unequal dispersion coefficients,” *Phys. Rev. E* **91**, 012924 (2015).
- ¹⁴E. G. Charalampidis, P. G. Kevrekidis, D. J. Frantzeskakis, and B. A. Malomed, “Vortex-soliton complexes in coupled nonlinear Schrödinger equations with unequal dispersion coefficients,” *Phys. Rev. E* **94**, 022207 (2016).
- ¹⁵E. Allgower and K. Georg, *Numerical Continuation Methods: An Introduction*, Vol. 13 (Springer-Verlag, Berlin, 1990).
- ¹⁶B. Malomed and Y. Stepanyants, “The inverse problem for the Gross–Pitaevskii equation,” *Chaos* **20**, 01313 (2010).
- ¹⁷F. Cooper, A. Khare, S. Charalampidis, J. Dawson, and A. Saxena, “Stability of exact solutions of the (2+1)-dimensional nonlinear Schrödinger equation with arbitrary nonlinearity parameter κ ,” *Physica Scripta* **98**, 015011 (2022).
- ¹⁸F. Cooper, A. Khare, J. F. Dawson, E. G. Charalampidis, and A. Saxena, “Uniform-density Bose-Einstein condensates of the Gross-Pitaevskii equation found by solving the inverse problem for the confining potential,” *Phys. Rev. E* **107**, 064202 (2023).
- ¹⁹G. H. Derrick, “Comments on nonlinear wave equations as models for elementary particles,” *J. Math. Phys.*, 1252–1254 (1964).
- ²⁰N. N. Bogolyubov, “On the theory of superfluidity,” *Izv. Akad. Nauk SSSR, Ser. Fiz.* **11**, 77–90 (1947).
- ²¹P. G. de Gennes, *Superconductivity of Metals and Alloys*, Vol. 86 (Benjamin, New York, 1966).
- ²²A. Gaidoukov and J. Anglin, “Bogoliubov-de Gennes theory of the snake instability of gray solitons in higher dimensions,” *Phy. Rev. A* **103**, 013319 (2021).
- ²³J. Satsuma and N. Yajima, “B. Initial Value Problems of One-Dimensional Self-Modulation of Nonlinear Waves in Dispersive Media,” *Progress of Theoretical Physics Supplement* **55**, 284–306 (1974), <https://academic.oup.com/ptps/article-pdf/doi/10.1143/PTPS.55.284/5392745/55-284.pdf>.
- ²⁴H. F., “New development in freefem++,” *J. Num. Math.* **20**, 251–266 (2012).
- ²⁵R. B. Lehoucq, D. C. Sorensen, and C. Yang, *ARPACK Users’ Guide* (Society for Industrial and Applied Mathematics, 1998).